INL/CON-08-14412
PREPRINT

Results of Tests to Demonstrate a Six-Inch-Diameter Coater for Production of TRISO-Coated Particles for Advanced Gas Reactor Experiments

ASME 4th International Topical Meeting on High Temperature Reactor Technology

Charles M. Barnes
Douglas W. Marshall
John Hunn
Bruce L. Tomlin
Joe T. Keeley

September 2008

4th International Topical Meeting on High Temperature Reactor Technology
HTR-2008
September 28-October 1, 2008, Washington DC, USA

HTR2008-58074

RESULTS OF TESTS TO DEMONSTRATE A SIX-INCH-DIAMETER COATER FOR PRODUCTION OF TRISO-COATED PARTICLES FOR ADVANCED GAS REACTOR EXPERIMENTS

Charles M. Barnes
Idaho National Laboratory
Idaho Falls, Idaho, USA

Douglas W. Marshall
Idaho National Laboratory
Idaho Falls, Idaho, USA

John Hunn
Oak Ridge National Laboratory
Oak Ridge, Tennessee, USA

Bruce L. Tomlin
Babcock & Wilcox
Lynchburg, Virginia, USA

Joe T. Keeley
Babcock & Wilcox
Lynchburg, Virginia, USA

ABSTRACT

The Next Generation Nuclear Plant (NGNP)/Advanced Gas Reactor (AGR) Fuel Development and Qualification Program includes a series of irradiation experiments in Idaho National Laboratory's (INL's) Advanced Test Reactor. TRISO-coated particles for the first AGR experiment, AGR-1, were produced at Oak Ridge National Laboratory (ORNL) in a two-inch diameter coater. A requirement of the NGNP/AGR Program is to produce coated particles for later experiments in coaters more representative of industrial scale. Toward this end, tests have been performed by Babcock and Wilcox (B&W) in a six-inch diameter coater. These tests are expected to lead to successful fabrication of particles for the second AGR experiment, AGR-2.

While a thorough study of how coating parameters affect particle properties was not the goal of these tests, the test data obtained provides insight into process parameter/coated particle property relationships. Most relationships for the six-inch diameter coater followed trends found with the ORNL two-inch coater, in spite of differences in coater design and bed hydrodynamics. For example the key coating parameters affecting pyrocarbon anisotropy were coater temperature, coating gas fraction, total gas flow rate and kernel charge size. Anisotropy of the outer pyrolytic carbon (OPyC) layer also strongly correlates with coater differential pressure.

In an effort to reduce the total particle fabrication run time, silicon carbide (SiC) was deposited with methyltrichlorosilane (MTS) concentrations up to 3 mol %. Using only hydrogen as the fluidizing gas, the high concentration MTS tests resulted in particles with lower than desired SiC densities. However when hydrogen was partially replaced with argon, high SiC densities were achieved with the high MTS gas fraction.

INTRODUCTION

Production of TRISO particles using an industrial-scale coater must be demonstrated in order to develop and qualify fuel for the NGNP Reactor [1]. High quality TRISO-coated particles for the AGR-1 irradiation experiment were produced by ORNL in a two-inch diameter coater. For AGR-2, an existing 6-inch diameter coater was chosen to demonstrate industrial-scale coated particle production [2]. A separate study evaluated coater crucible and gas distributor designs and recommended initial designs to test [3].

Following modifications to the coating process at B&W facilities [4], 21 partial or full coating tests were performed using 400-µm yittria stabilized zirconia (YSZ) surrogate kernels and then 16 tests using 520-µm YSZ kernels [5]. The larger surrogate kernel was used so that after applying a buffer layer of about 50 µm, hydrodynamic similarity to UCO kernels would be achieved for the final three coating layers. In the final phase of testing, natural uranium UCO kernels were coated so that SiC defects in resulting coated particle batches

could be determined using the burn-leach method. Twenty-one TRISO coating runs were made with natural uranium UCO kernels prior to coating low enriched uranium kernels to obtain particles for the AGR-2 irradiation experiment.

The coater tests had three purposes. The first purpose was to demonstrate a coater design and determine coating conditions that produce particles meeting all AGR-2 fuel specifications. The second purpose was to provide data for selection of variant coating conditions for AGR-2 fuel. Fuel for the AGR-1 experiment includes particles made with the IPyC layer applied at two temperatures and two coating gas fractions, and the SiC layer applied with and without argon dilution. Plans for the AGR-2 test also include fuel with particles having SiC layers produced with methyltrichlorosilane (MTS) in hydrogen only and, in a separate capsule, fuel with particles having SiC deposited with MTS in an argon-hydrogen mixture. Substituting argon for a portion of the hydrogen during silicon carbide coating has been reported in coating literature to offer advantages of less severe coating conditions without compromising SiC layer properties [6]. The third purpose of the coater tests was to obtain and evaluate pressure fluctuation data as a real-time indicator of coater fluid dynamics and to determine if pressure data could be correlated with particle properties.

Two other papers presented in this conference focus on B&W coater test results that achieved these three purposes, and include descriptions of the coater [7, 8]. This paper reviews all of the test data and compares coating parameter trends with those from the AGR-1 coater.

EXPERIMENTAL

The coater tube used to produce AGR-1 particles was 2-inches in diameter and had a conical gas distributor. The gas inlet was water cooled. Further details of the AGR-1 coater are given in Reference 9.

The B&W coater has a 6-inch diameter tube and a multi-holed gas distributor. A liquid cooled inlet was used in some early tests but showed no significant benefits and so was not used in later tests. Additional details of the B&W coater are given in Reference 7. Total gas flow rates for the B&W coater were approximately 19-20 times the flow rates of the 2-inch coater for the buffer and IPyC layers and 11-13 times the flow rates of the smaller coater for the SiC and OPyC layers.

For both coaters, coatings were applied without interruption, that is, without stopping at any intermediate point to cool, unload and sample the partially-coated particles to obtain quality control (QC) measurements. The B&W coater has a hot sampler that can be used to take two 2-cm^3 samples per run. Typically two samples of either buffer-coated or inner pyrolytic carbon (IPyC)-coated particles were taken during a coating run.

Layer thicknesses and particle aspect ratios were measured using photographs of ceramographic mounts of coated particles and image analysis software developed by ORNL [10].

Two methods were used to determine densities of the buffer layer. In both methods mercury porosimetry was used to determine the volume or density of a sample of buffer coated particles. In early tests B&W calculated the buffer density using measurements of buffer particle density, kernel diameter, buffer thickness and kernel density. For ORNL and later buffer density measurements at B&W, the average weight of buffer-coated particles was determined using multiple samples. Using this average weight and the mass of the porosimeter sample, an average number of particles in the buffer-coated sample was calculated. From the sample volume measured by the porosimeter and the number of particles in the sample, the volume per particle was calculated. The same measurements were made on uncoated kernels. The mass per particle and volume per particle of the buffer coating were determined by subtraction, and the buffer density then calculated from these differences.

Pyrocarbon and SiC densities were determined using sink-float density columns. Pyrocarbon anisotropies were measured using an ellipsometry method developed at ORNL [11]. Pyrocarbon surface connected porosities were determined by mercury porosimetry over a pressure range of 250-10,000 psi. The burn leach method was used to determine SiC defects. SiC inclusions and the missing OPyC layer defect fraction were determined by visual examination of ceramographic mounts and loose particles respectively.

BUFFER LAYER

Specifications for the buffer layer of AGR-2 particles include a density of 1.05±0.10 g/cm^3 and a thickness of 100±15 µm. For a given coater charge and coating gas, the primary coating parameter that determines the buffer layer density is the partial pressure of coating gas [6, 12-13]. The buffer layer was applied to AGR-1 fuel particles using an acetylene to total gas (acetylene plus argon) ratio of 0.6, a coating gas flow rate of 8.5 standard liters per minute (slpm), and a temperature of 1450ºC. These conditions gave an average coating rate of 21 µm/min. and a buffer density of 1.1 g/cm^3. The laboratory AGR-1 coater had the capability to control the temperature with a cooling jacket during the exothermic reaction of buffer coating.

Similar conditions in the B&W coater gave similar densities. Using the same coating gas fraction (0.6) and a total gas flow rate of typically 162 slpm (corresponding to about the same average coating rate [22-24 µm/min]), particles with buffer densities of 0.94-1.1 g/cm^3 were obtained. Typically, the bed temperature for the B&W coater increased by about 130ºC during buffer coating, from a temperature of 1370ºC at the start of buffer coating to a temperature near 1500ºC at the end of the

coating. Temperature in the B&W coater is controlled by a thermocouple located near the outer surface of the coating tube. The above typical temperature rise during buffer coating corresponds to a control temperature of 1470ºC.

Buffer samples were taken for density analysis from 22 B&W coating runs. For these runs the coating gas fraction varied from 0.54 to 0.60, the total gas flow rate from 102 to 186 slpm, the average coating rate from 12 to 25 µm/min, and the control temperature from 1400 to 1520ºC. For three runs in which the buffer layer was applied with low coating rates and low temperatures, the buffer density was found to be 0.88-0.90 g/cm^3. However at all other conditions, buffer densities were 0.94-1.16 g/cm^3.

PYROLYTIC CARBON LAYERS

AGR fuel specifications for pyrocarbon layers include layer densities (1.90±0.05 g/cm^3), thicknesses (40±4 µm), and anisotropies (mean equivalent $BAF_o \leq 1.045$ for IPyC and $\leq$ 1.035 for OPyC). The mean equivalent BAF_o, calculated as 1+ 3 times the diattenuation, is used in order to compare results to historical German particle anisotropy values. Although not a specification, the surface connected porosity of the pyrocarbon layers is also an important property and was measured for samples from many of the coating tests.

AGR-1 fuel includes particles with IPyC layers deposited at three different coating conditions:

Fuel	Coating Temperature	Coating Gas Fraction
Baseline	1265ºC	0.3
Variant 1	1290ºC	0.3
Variant 2	1265ºC	0.45

Due to the IPyC layer being applied at a higher temperature, variant 1 particles have a lower IPyC density and a lower anisotropy than baseline particles. Increasing the coating gas fraction, as was done for variant 2 particles, is an alternative means of increasing the coating rate and generally results in a lower anisotropy [14]. However, for the AGR-1 particles, the anisotropies of baseline particles and variant 2 particles were nearly equivalent (0.0074 diattenuation for baseline particles compared to 0.0075 for variant 2 particles).

Prior to fabrication of AGR-1 particles, a study was performed in which IPyC coating temperatures and gas fractions were systematically varied [15]. Consistent with previous fuel coating literature [6, 12-13], pyrocarbon density was found to be primarily dependent on bed temperature. A comparison of the trends of pyrocarbon density versus temperature for the two-inch and six-inch diameter coaters is shown in Figure 1.

Interestingly, for the IPyC layer (the green and black data points and trend lines of Figure 1), the trend lines for the two coaters intersect very near to a density of 1.9 g/cm^3, which is the target density for AGR fuel. The trend line for the IPyC density of particles produced in the six-inch diameter coater has a lower slope than the IPyC density trend line for the two-inch coater; hence acceptable IPyC densities can be obtained with the larger coater over a wider temperature range. The same is true for the OPyC layer. These trends likely reflect differences in temperature profiles between the two coaters.

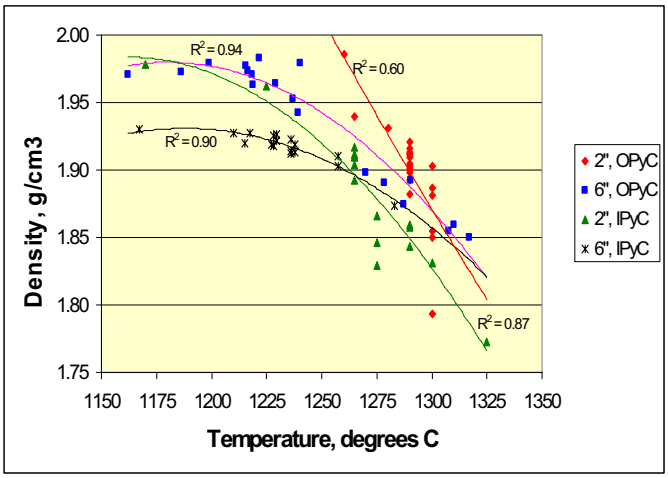

Figure 1. Comparison Of Pyrocarbon Density Versus Temperature For 2" And 6" Diameter Coaters

Figure 1 also shows that to achieve the same OPyC density as IPyC density, a higher temperature is required, at least up to a temperature of about 1325ºC. The scatter in the data shown in Figure 1, such as the range of OPyC densities for the two-inch diameter coater at 1300ºC, illustrates the fact that coater temperature measurements have uncertainties. Internal thermocouples, external thermocouples and pyrometers all have limitations.

Figure 2 shows data only for the B&W coater. Densities plotted against bed temperature (the green and blue data points and trend lines) are the same as shown on Figure 1. The other two data sets shown on Figure 2 are densities plotted versus coater control temperatures. Figure 2 shows that to have high confidence in meeting the density specification, a control temperature in the range 1175-1340ºC is needed for the IPyC layer, while the narrower range of 1335-1365ºC is needed for the OPyC layer.

Past studies have shown that the anisotropy of pyrocarbon layers decreases with increasing coating temperature and increasing coating rate [12, 14, 16]. Figure 3 shows trends of equivalent anisotropy versus temperature, coating gas fraction,

and average coating rate[1] for the two-inch diameter coater used to produce AGR-1 particles. The AGR-1 coating data confirms the trend of decreasing anisotropy with increasing coating temperature, but indicates that for any temperature, there is an optimum coater rate that gives a minimum anisotropy. Furthermore, there is an optimum coating gas fraction that appears to be nearly independent of temperature. For the AGR-1 coater, this optimum coating gas fraction is about 0.35.

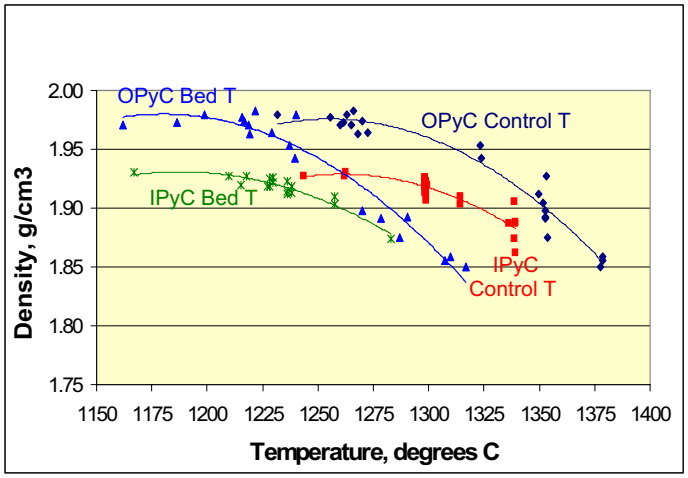

Figure 2. Pyrocarbon Densities Versus Bed And Control Temperatures For 6" Coater

Figure 4 shows equivalent anisotropy plotted against temperature. With two exceptions, all data plotted in Figure 4 is for particles produced with a coating gas fraction in the range of 0.28-0.32.

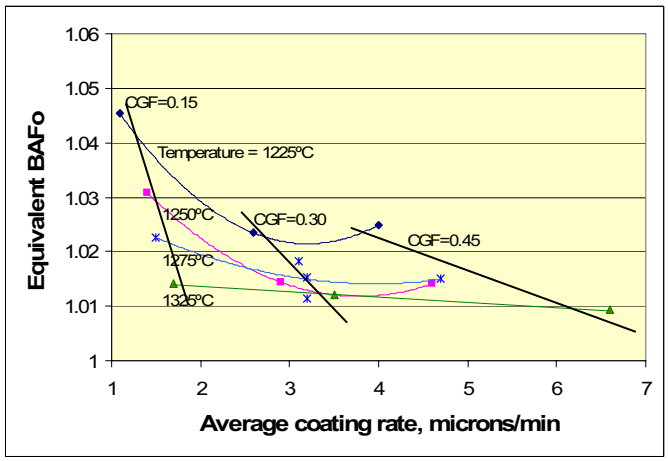

Figure 3. Pyrocarbon Anisotropy Versus Coating Parameters

At all temperatures, the IPyC anisotropy is greater for particles produced in the six-inch coater than those produced in the two-inch coater. As shown by the red data points in Figure 4, increasing the coating gas fraction (to 0.40) or total gas flow rate (by 14%) during IPyC coating increased the layer anisotropy for the large coater. However, these alternative conditions were tested in only one run each; hence caution is advised in drawing any conclusions from this limited data.

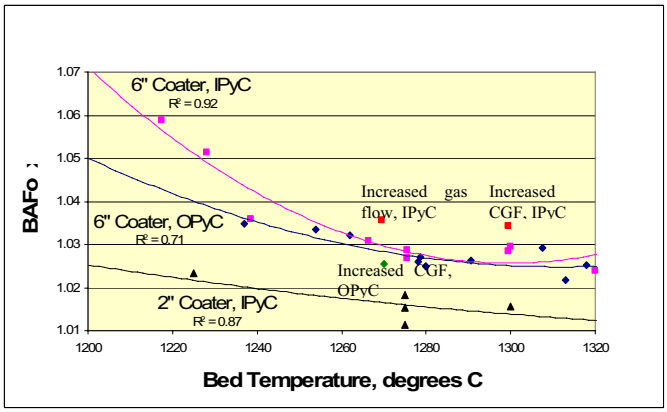

Figure 4. Pyrocarbon Anisotropy Versus Coating Temperatures

Figure 4 also compares IPyC and OPyC anisotropies for the six-inch coater. At temperatures lower than about 1250ºC, the OPyC anisotropy is clearly lower than that for the IPyC layer. At higher temperatures, there appears to be only a small difference between IPyC and OPyC anisotropy. For AGR fuel, pyrocarbon anisotropy specifications push coating temperatures to the maximum that will still result in acceptable layer densities. Since the upper temperature limit for acceptable density is higher for the OPyC layer than the IPyC layer, the OPyC layer is typically deposited at a higher temperature than the IPyC layer and anisotropies are thus lower for the OPyC layer than for the IPyC layer. Hunn has also reported that IPyC exposure to the higher temperature SiC coating results in an increase in IPyC anisotropy [17]. As shown by the green data point in Figure 4, and contrary to the results for the IPyC layer, an increase in the coating gas fraction for OPyC resulted in a decrease in the layer anisotropy.

While most anisotropy results for the six-inch coater can be explained based on coating conditions, results for two runs (tests 93046 and 93055) do not fit trends for variation of anisotropy with temperature, coating gas fraction or coating rate. In an effort to explain these results, the anisotropy data was plotted against additional coating parameters. When plotted versus coater differential pressure (Figure 5), one of the anomalous points fell in line with much but not all of the remaining data. Plotted versus the coater inlet pressure at the end of the run (Figure 6), both anomalous data points fit the general trend, although the correlation (r^2) is not as good. These data suggest coater pressure parameters may affect pyrocarbon anisotropy.

[1] Coating rate varies with time during any coating. Coating rates plotted in Figure 3 and later figures have not been adjusted for small variations in layer thicknesses observed in the difference tests.

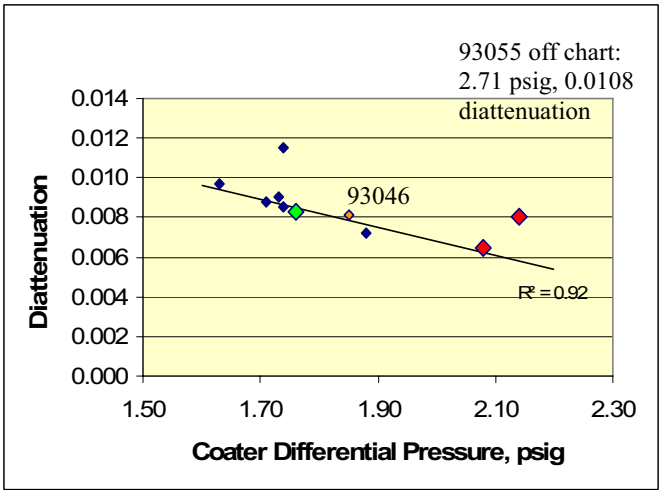

Figure 5. OPyC Diattenuation Versus Coater Differential Pressure

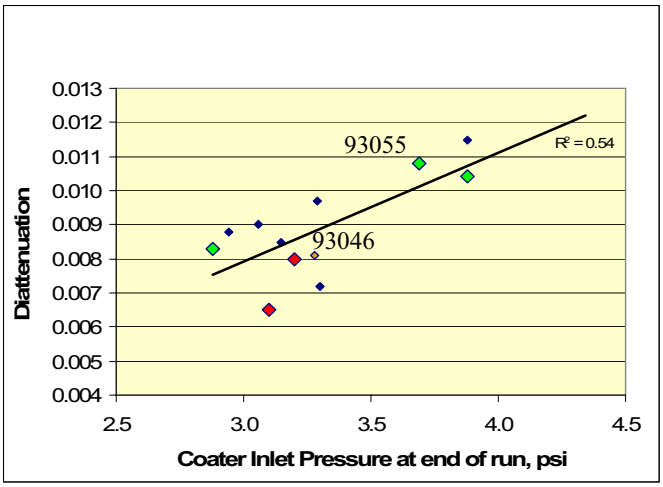

Figure 6. OPyC Diattenuation Versus Coater Inlet Pressure

A third important pyrocarbon property is the surface connected porosity. An IPyC surface connected porosity greater than about 1.3 ml/m^2 is desired to ensure a good bond between the IPyC and SiC layer. An OPyC porosity of the same magnitude is desired to minimize OPyC failure during irradiation [18]. AGR-1 coating tests showed that the IPyC surface connected porosity increased with increasing temperature and increasing coating gas fraction [15]. Figure 7 compares IPyC surface connected porosities versus coating rate for the two-inch and six-inch coaters. Trend lines for the two sets of data intersect at a porosity of 1 ml/m^2. The increase in porosity with increasing coating rate is slightly greater for the six-inch coater than the two-inch coater, which will result in a higher IPyC surface connected porosity for AGR-2 particles than for AGR-1 particles. The IPyC porosity expected for AGR-2 particles is 2.0-2.2 ml/m^2.

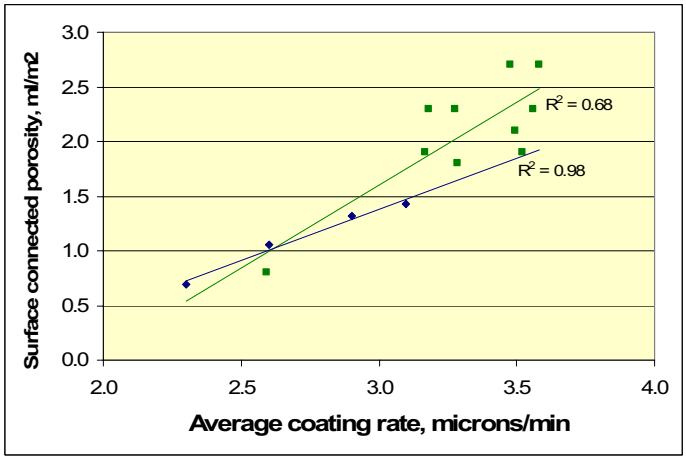

Figure 7. Comparison Of IPyC Surface Connected Porosities For The Two Coaters

Figure 8 shows surface connected porosity data for both the IPyC and OPyC layers and for both coaters. The effect of coating gas fraction on IPyC porosity can be seen in comparing data for the two-inch coater at coating gas fractions of 0.15, 0.3 and 0.45 (dark blue diamond, purple square and yellow triangle data points). The comparison of OPyC layer surface connected porosity for the two coaters is less straight forward than the comparison for the IPyC layer. An OPyC layer coating rate of about 4.0 µm/min was achieved for the two-inch coater by using a coating gas flow rate about 170% of that used for the IPyC layer. The coating gas fraction for both pyrocarbon layers was the same (0.30), while the OPyC coating temperature was 25ºC higher than that for the IPyC layer. These conditions resulted in porosities of 0.95-1.3 ml/m^3 for each pyrocarbon layer for particles produced in the two-inch coater.

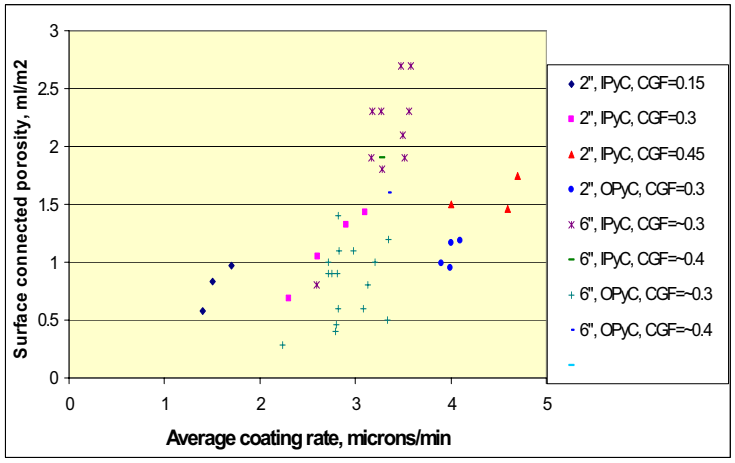

Figure 8. Pyrocarbon Surface Connected Porosity Versus Average Coating Rate

The OPyC data for particles produced in the larger coater show more scatter, in part reflecting variations in OPyC flowrates, temperatures, and coating gas fractions used in the various tests. However, for both coaters it is clear that at

equivalent coating rates, OPyC surface connected porosities are significantly lower than those for the IPyC layer at equivalent coating conditions, and increasing OPyC temperature alone is not sufficient to increase the OPyC porosity to values above 1.3 ml/m^2. In three tests of the 6-inch coater, OPyC samples were taken from the coater bed after OPyC coating but prior to cooling. The hot samples of OPyC particles were analyzed to see if post-coating activities (cooling, unloading, sieving and tabling) modify the particle surface so as to reduce the OPyC surface connected porosity. In all three cases the porosity of the hot sample was higher than that of the bulk particle sample. These results are shown in Table 1.

Table 1. Comparison of surface connected porosities of hot and bulk OPyC samples

Test	Porosity, ml/m2	
	Hot Sample	Buk Sample
93063	0.9	0.8
93065	0.7	0.4
93069	0.9	0.6

SILICON CARBIDE LAYER

Specifications for the silicon carbide layer include the thickness, density, a maximum defect fraction as measured by the burn-leach method, the SiC-coated particle aspect ratio, the SiC grain size and the "gold spot" defect fraction. The usual method for gold spot analysis, optical analysis of particles burned back to the SiC layer, was found inadequate to accurately detect these SiC anomalies for particles with small-grained microstructure. So to evaluate particles against this specification, particles were sectioned and examined for soot inclusions in the SiC layer.

Figure 9 shows SiC density results for a number of 6" coating tests made at different concentrations of methyltrichlorosilane (MTS), concentrations of argon, and coating temperatures. For tests using hydrogen only as the fluidization and dilution gas, the SiC layer density decreased with increasing MTS concentration. Higher MTS concentrations have the economic advantage of reduced coating times.

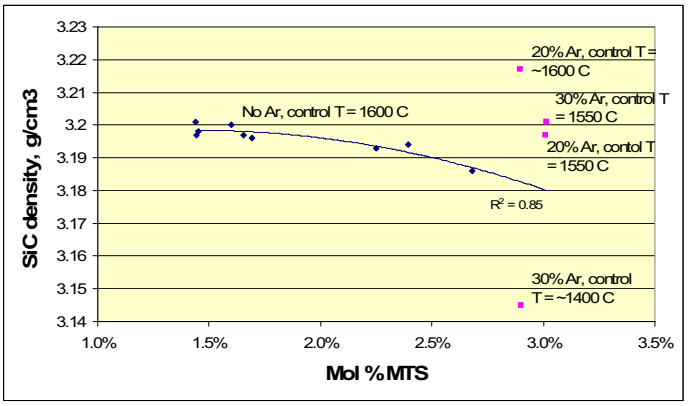

Figure 9. SiC Density Versus Coating Parameters

High density (>3.19 g/cm^3) SiC was obtained with 3% MTS when a hydrogen-argon mixture was used to fluidize the particle bed and the control temperature was greater than 1550ºC. Near theoretical density SiC was obtained using a gas mixture of 20% Ar/80%H_2 containing 3% MTS and a coater control temperature of 1600ºC. At a control temperature of 1550ºC, particles with SiC densities near 3.2 g/cm^3 were obtained with gas mixtures of 20-30% argon. At this temperature, the SiC density for the test with 30% argon was slightly higher than the test with 20% argon. Lowering the control temperature to 1400ºC resulted in particles with SiC densities of only 3.145 g/cm^3. Low density SiC from the test at 1400^{o}C was not analyzed for the presence of free Si or free C. Compared to the traditional method of depositing SiC with hydrogen only, partial substitution with argon both allowed for using higher MTS concentrations and reduced coating temperatures to achieve the desired SiC density.

Figures 10A-D compare the SiC microstructure of particles from both coaters. The largest grains are seen for particles produced in the 2-inch coater at a temperature of 1500^{o}C, an MTS concentration of 1.5% and hydrogen only as the fluidization gas. Partial replacement of hydrogen with argon resulted in achieving the same desired SiC density at a temperature of 1425^{o}C and a smaller grain size.

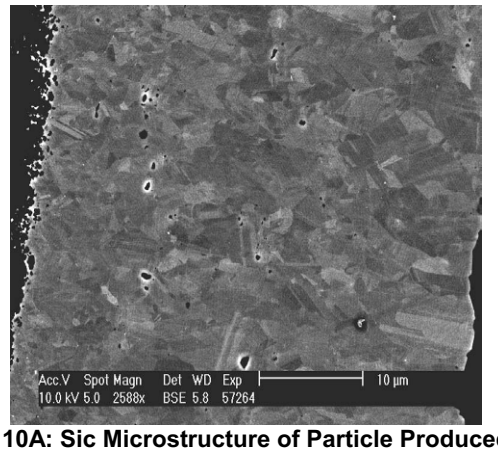

Figure 10A: Sic Microstructure of Particle Produced In 2" Coater With H_2 Only, 1.5% MTS, And 1500ºC Bed Temperature

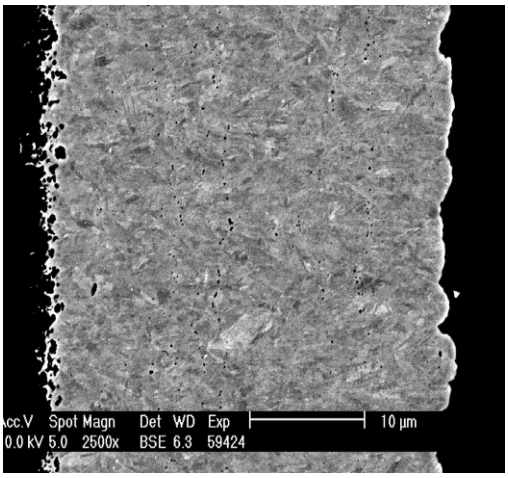

Figure 10B: Sic Microstructure of Particle Produced in 2" Coater With 50% Ar, 2% MTS, And 1425ºC Bed Temperature

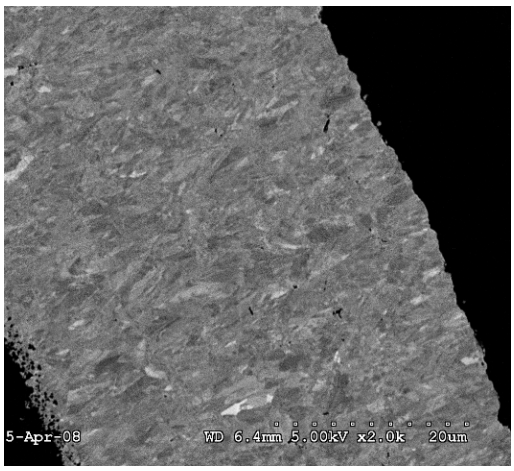

Figure 10c. SiC Microstructure of Particle Produced In 6" Coater Using H_2 Only, 1.5% MTS, And 1600ºC Coater Control Temperature (~1470ºC Bed Temperature)

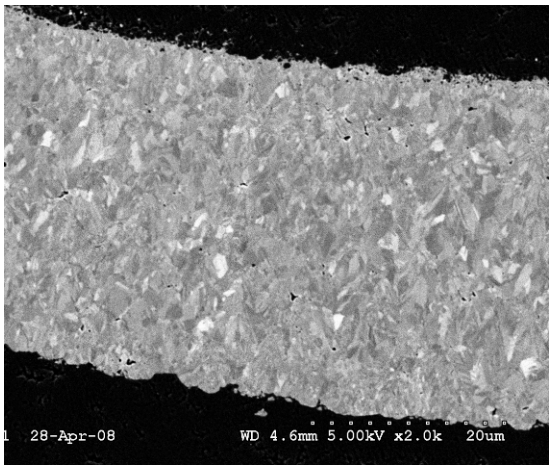

Figure 10D. SiC Microstructure of Particle Produced In 6" Coater Using 30% Ar, 3% MTS, And 1550ºC Coater Control Temperature (~1425ºC Bed Temperature)

For the 6-inch coater, it was found that a slightly lower temperature (~1470°C) than used in the small coater could achieve adequate layer density and a smaller grain size for the hydrogen only-case. The SiC grain size for particles from the two coaters is similar when argon dilution is used.

Lenticular flaws in SiC coatings have been reported in particles from ORNL, General Atomics and Japanese coaters [9, 19-21]. Typically observed as gold-colored areas on particles burned back to the SiC layer, examination of cross-sectioned particles show that these flaws are circumferential inclusions of low density SiC or carbon. Minimizing these flaws in AGR-1 particles involved controlling gas flowrates within a very narrow range. However, while an occasional SiC inclusion has been seen in images of particles coated in the B&W 6-inch coater (Figure 11), examination of samples of about 12,000 particles from two later runs by cross sectioning showed only 1 particle with an inclusion. It is believed that the design of the B&W coater with a relatively long tube is the primary cause for the significant reduction in SiC flaws for this coater compared to the AGR-1 coater. The longer tubes prevent particles from contact with cooler surfaces where SiC soot is deposited during coating.

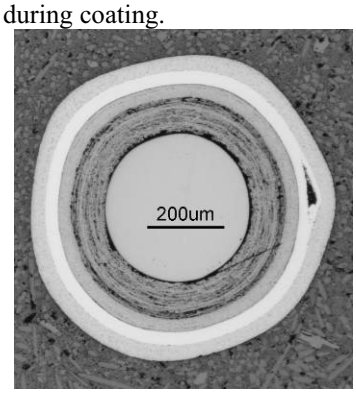

Figure 11. Example of SiC Inclusion In Particle From B&W Coating Run 93019

SiC defects include radial cracks in the SiC layer, broken particles, missing SiC layers or other anomalies that compromise the structural integrity of the layer. AGR particle specifications allow only 1 defective particle out of a sample of 50,000 particles, or 14 defects out of a sample of 220,000. SiC defects for the AGR-1 particles were very low, with 0 or 1 defects found in samples of 120,000 particles for three of the AGR-1 fuels and 1 defect found in a sample of 50,000 particles for the fourth fuel.

The level of defects in particles from the 6-in coater has varied widely. The specification for SiC defects has been met for particles from 12 out of 20 runs. The level of SiC defects does not correlate with any coating parameter, but, as shown in Figure 12, most coating runs resulting in particles with higher levels of SiC defects had thinner SiC layer thicknesses. Low levels of SiC defects were achieved in the final five consecutive coating tests by ensuring that the layer thickness was at least 35 µm and also by careful particle upgrading (sieving and tabling).

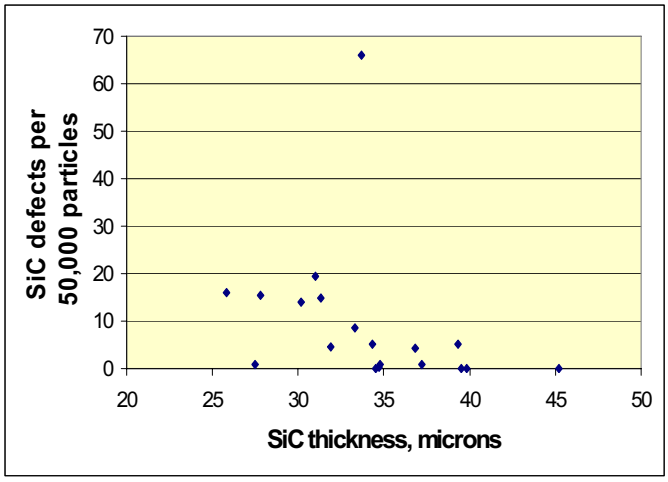

Figure 12. Correlation of SiC Defects with Coating Thickness

A final characteristic of the SiC layer, while not a specification, relates to the bonding of the layer with the IPyC layer. As identified by Petti et al [22, 23], interlacing of these two layers is desired in order to achieve a strong bond. Localized debonding can lead to stress intensification during irradiation and possible failure. Figure 13 shows an example of this interface for a particle coated in the 6-inch furnace by B&W. The relatively high IPyC surface porosity results in SiC infiltration during coating, which gives the desired strong interface.

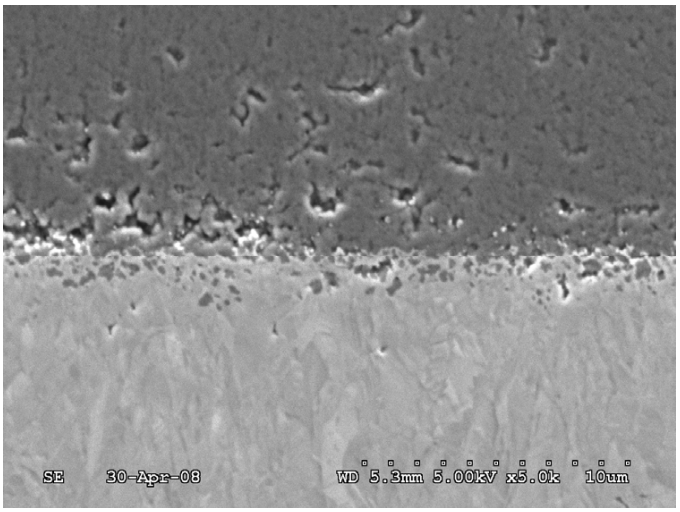

Figure 13. Example of IPyC-Sic Interface Showing Interlacing of the Two Layers

CONCLUSIONS

Demonstration tests of a six-inch fluidized bed CVD coating furnace have provided data that has been used to prepare for coating particles for AGR-2 fuel. The tests have demonstrated a coater design and coating process parameters needed to meet particle specifications. Most trends of particle property relationships with coating parameters were found to be very similar to those determined for a 2-inch laboratory coater, but a few exceptions were found. Besides determining specific coating parameters for AGR-2 baseline and variant particles, the test data has provided information as to how tightly these parameters must be controlled.

ACKNOWLEDGMENTS

This manuscript has been authored by Battelle Energy Alliance, LLC under Contract No. DE-AC07-05ID14517 with the U.S. Department of Energy. The authors wish to thank the operators at B&W that performed the coating test and researchers at ORNL that supported particle characterization. The United States Government retains and the publisher, by accepting the article for publication, acknowledges that the United States Government retains a nonexclusive, paid-up, irrevocable, world-wide license to publish or reproduce the published form of this manuscript, or allow others to do so, for United States Government purposes.

REFERENCES

[1] Petti, D., Hobbins, R., Kendall, J., Saurwein, J., 2005, *Technical Program Plan for the Advanced Gas Reactor Fuel Development and Qualification Program*, INL/EXT-05-00465, Revision 1.

[2] Barnes, C. M., Marshall, D. W., 2006, *Advanced Gas Reactor Coater Scale Up Plan*, PLN-1975, Revision 0 (distribution of this document is limited).

[3] Marshall, D. W., 2006, *Six-Inch TRISO Fuel Coater Design for AGR-2*, EDF-6666, Revision 1 (distribution of this document is limited).

[4] Marshall, D. W., Barnes, C. M, 2007, *AGR Fuel Development – Coater and Control System Upgrade*, INL/EXT-07-12458.

[5] Barnes, C. M., Marshall, D. W, 2007, *FY 2007 Six-inch Diameter Coater Test Report*, INL/EXT-07-13090.

[6] Ford, L. H., Hibbert, N. S., Martin, D. G., 1972-3, "Recent Developments of Coatings for GCFR and HTGCR Particles and Their Performance," *J. Nuclear Materials 45*, pp. 139-149.

[7] Keeley, J. T., Tomlin, B. L., 2008, "Development of a Continuous CVD Process for TRISO Coating of AGR Fuel," *Proceedings of the 4th International Topical Meeting on High Temperature Reactor Technology*, Paper HTR2008–58008

[8] Marshall, D. W, Barnes, C. M., 2008, "Mining Process and Product Information from Pressure Fluctuations within a Fuel Particle Coater," *Proceedings of the 4th International Topical Meeting on High Temperature Reactor Technology*, Paper HTR2008–58073.

[9] Lowden, R. A., 2006, *Fabrication of Baseline and Variant Particle Fuel for AGR-1*, ORNL/CF-06/02.

[10] Kercher, A. K., Hunn, J. D., Price, J. R., Jellison, G. E., Montgomery, F. C., Morris, R. N., Giaquinto, J. M., Denton, D. L., 2005, Advanced Characterization Methods for TRISO Fuels, Proceedings of the Advanced Reactors with Innovative Fuels Workshop (ARWIF-2005), February 2005.

[11] Jellison, G. E., Jr.., Hunn, J. D., Lowden, R. A., 2006, "Optical Characterization of Tristructural Isotropic Fuel Particle Cross-Sections Using Generalized Ellipsometry," *J. Nuclear Materials 352*, pp. 6-12

[12] Pratt, B., Sease, J. D., Pechin, W. H., Lotts, A. L., 1969, "Pyrolytic Carbon Coating in and Engineering-Scale System," *Nuclear Applications 6*, pp. 241-255.

[13] Charollais, F., Fonquernie, S., Perrais, C., Perez, M., Dugne, O., Cellier, F., Harbonnier, G., Vitali, M.-P., 2006, "CEA and AREVA R&D on HTR Fuel Fabrication and Presentation of the CAPRI Experimental Manufacturing Line," *Nuclear Engineering and Design 236*, pp. 534-542.

[14] Stinton, D. P., Thiele, B. A., Lackey, W. J., Morgan, C. S., 1982, "Detection and Control of As-Produced Pyrocarbon Permeability in Biso-Coated HTGCR Fuel Particles," *Ceramic Bulletin 61*, pp. 245-250.

[15] Lowden, R. A., Hunn, J. D., Nunn, S. D., Kercher, A. K., Price, J. R., Menchhofer, P. A., Jellison, Jr., G. E., 2005, *Effects of Deposition Conditions on the Properties of Pyrolytic Carbon Deposited in a Fluidized Bed*, ORNL/TM-2005/533.

[16] Lackey, W. J., Stinton, D. P., Sease, J. D., 1977, "Improved Gas Distributor for Coating HTGCR Fuel Particles," *Nuclear Technology 35*, pp. 227-238.

[17] Hunn, J. D., Jellison, Jr., G. E., Lowden, R. A., 2008, " Increase in Pyrolytic Carbon Optical Anisotropy and Density During Processing of Coated Particle Fuel Due to Heat Treatment," *J. of Nuclear Materials 374*, pp. 445-452.

[18] Bullock, R. E., Historical Review of Coated-Particle Fuel as Related to the Performance of TRISO-P Particles, 1993, CEGA Interoffice Correspondence, CEGA-M-93-1274.

[19] Scott, C. B., 1971, "Carbon Inclusions in SiC Coatings of FSV Production Fuel Particles," General Atomics Memorandum CBS-014-FMB-71.

[20] Saurwein, J., 1992, "Characterization of Gold Spots in NPR Performance Test Fuel SiC Coatings," General Atomics Document 910523.

[21] Minato, K., Kikuchi, H., Fukuda, K., Suzuki, N., Tomimoto, H., Kitamura, N., Kaneko, M., 1994, "Internal Flaws in the Silicon Carbide Coatings of Fuel Particles for High-Temperature Gas-Cooled Reactors," *Nuclear Technology 106*, pp. 342-349.

[22] Petti, D. A., Buongiorno, J., Maki, J. T., Hobbins, R. R., Miller, G. K., 2003, "Key Differences in the Fabrication, Irradiation and High Temperature Accident Testing of US and German TRISO-Coated Particle Fuel, and their Implications on Fuel Performance," *Nuclear Engineering and Design 222*, pp. 281-297.

[23] Miller, G. K, Petti, D. A., Maki, J. T., 2004, "Considerations of the Effects of Partial Debonding of the IPyC and Particle Asphericity on TRISO-Coated Fuel Behavior," *J. of Nucl. Materials 334*, pp. 79-89.